Resonant Phonon Scattering by Radiation-Induced Crystal Defects in CaF_2

C. Wurster, K. Lassmann, and W. Eisenmenger
1. Physikalisches Institut, Universität Stuttgart, W-7000 Stuttgart 80, Germany
(Received 1 February 1993)

After irradiation of CaF_2 single crystals with electrons in the range of 500 keV to 1 MeV we find by phonon spectroscopy with superconducting tunneling junctions phonon scattering lines at 398 GHz and 628 GHz. The line strength at 398 GHz decreases with isochronal annealing correlated with the decrease of the optical absorption at 550 nm in these samples due to Ca clusters of an average radius of 6 nm. We ascribe the 398 GHz line to acoustic resonances of these clusters and the line at 628 GHz to resonant phonon scattering at localized excitons of F- and H-center pairs.

PACS numbers: 63.20.Mt, 46.30.My

In this Letter we report the first frequency resolved observation of resonant phonon scattering by Ca clusters in electron-irradiated CaF_2. Resonant scattering of elastic waves by objects of dimensions of the acoustic wavelength is an important topic of applied ultrasonics [1]. The practical lower dimensional limit of this technique is of the order of microns. There is, however, widespread practical and fundamental interest in the investigation of much smaller structures such as precipitates, clusters, or voids in, e.g., irradiated, ion implanted, or annealed solids. Resonant phonon scattering in this range of submicron dimensions has been investigated so far only by measurement of the thermal conductivity of, e.g., NaCl containing Ag clusters [2] and γ-irradiated LiF [3]. The analysis of the size distribution is limited by the width of the thermal spectrum. Significantly higher frequency resolution ($\sim$ 1 GHz) than with thermal conductivity is possible by phonon spectroscopy with superconducting Al and Sn tunneling junctions in the frequency range between 285 GHz and $\sim$ 3 THz as phonon generators and detectors [4, 5]. The average cluster size can be determined by the wavelength of resonant optical Mie scattering [6] induced by the excitation of surface plasmons. This kind of excitation was also measured in various ionic crystals containing small metal clusters using surface enhanced Raman scattering [7]. The analysis of the optical measurements has shown that e^- irradiation generates a relatively narrow size distribution of the clusters and, in addition, that there exists a complex system of balance between the Ca clusters and color centers, V_K centers, H centers, and dislocation loops. The point defects and Ca clusters can be identified by optical absorption in the visible range whereas dislocation loops are observable only with a transmission electron microscope (TEM) [8].

The samples were electron irradiated with energies between 550 and 900 keV and at irradiation temperatures of 4.2 K, $\sim$ 120 K, and $\sim$ 230 K with irradiation doses in the range from 5×10^{18} to 3×10^{19} cm^{-2}. γ and electron irradiation at liquid helium temperatures did not influence the phonon transmission [9]. On the other hand, as shown in Fig. 1, electron irradiation at temperatures above 100 K leads to the appearance of two phonon scattering dips at 398 GHz (1) and 628 GHz (2). Dip (3) at 756 GHz is present in all 7 samples which were obtained from different sources and is not influenced by the irradiation. To our knowledge no far infrared (FIR) absorption at this frequency has been observed so far. The steep signal rise at 285 GHz corresponds to the detector threshold ($2\Delta_{Sn} = h\cdot285$ GHz) and the hump in front of it to a thermal precursor of the Al generator.

Isochronal (1 h) annealing steps at temperatures between 570 and 720 K show that there is a correlated decrease of dip (1) at 398 GHz (Fig. 1) and the optical absorption at 550 nm due to Mie scattering (Fig. 2). A small shift of the minimum frequency with annealing temperature as visible in Fig. 1, however, has no observable correspondence in the optical scattering. The changes of dip (2) at 628 GHz with annealing temperature will be discussed below.

From this correlation we deduce that dip (1) at 398 GHz is due to resonant phonon scattering at

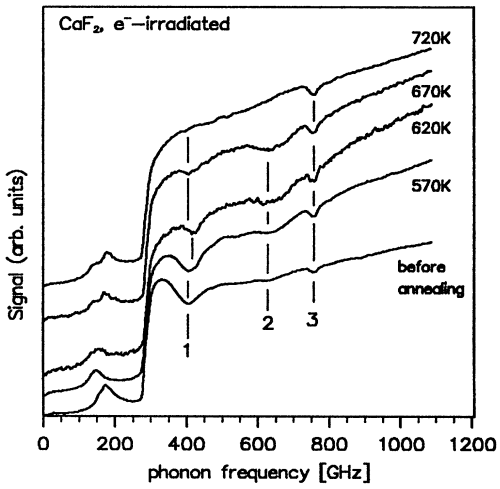

FIG. 1. Phonon transmission of electron-irradiated CaF_2 before and after stepwise isochronal annealing (1 h) in the range of 570 to 720 K.

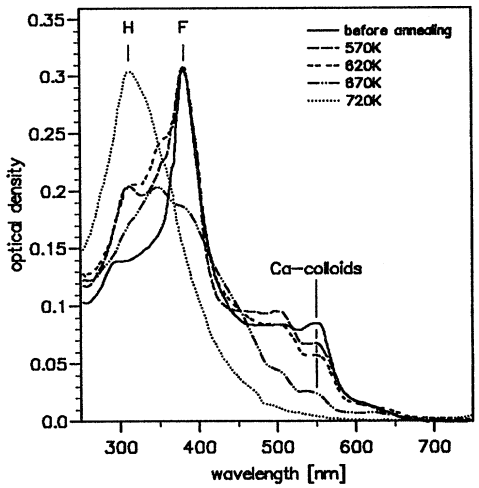

FIG. 2. Optical absorption spectra of electron-irradiated CaF_2 before and after stepwise isochronal annealing in the range of 570 to 720 K.

Ca clusters. Because of the stability of the position of the optical absorption due to Mie scattering at 550 nm with annealing we expect that the average cluster radius of 6 nm [6] and thus the acoustic scattering cross section of the individual cluster is not changed by annealing but instead the concentration of scatterers.

For a quantitative correlation we calculated the concentration of scatterers from both optical and acoustic measurements. In the case of optical absorption spectroscopy the area below the line due to resonant Mie scattering at 550 nm is proportional to the concentration of scatterers after the contribution of the nonresonant background scattering has been subtracted.

In the case of phonon transmission spectra we have to consider the possibility of elastic and inelastic scattering. After inelastic scattering the phonons will most probably have frequencies below the detector threshold of 285 GHz and are lost for a contribution to the signal if we assume that scattered phonons decay after down-conversion mainly into two phonons of the same energy [10]. With this assumption we obtain Beer's law for the inverse mean free path which depends linearly on the concentration of scatterers.

Elastically scattered phonons may arrive at the detector or pass by and get lost to the surrounding liquid helium. Thus one has to take into account the geometry of the generator, transmission path, and detector, and the acoustic anisotropy of the transmission medium (phonon focusing). By Monte Carlo simulation we obtain an effective damping as a function of the average elastic or inelastic scattering length [11]. It is obvious that inelastic scattering leads to much deeper dips as compared to elastic scattering of the same mean free path. We find a nonlinear logarithmic relation between the effective damping for the elastic case and the inverse mean free path. Since the inverse mean free path is proportional to the concentration of scatterers the effective damping describing elastic scattering is a nonlinear function of the concentration of scatterers. This different concentration dependence allows us to separate elastic from inelastic phonon scattering when we compare it with the values obtained by optical absorption spectroscopy.

We have fitted the results of the Monte Carlo calcula-

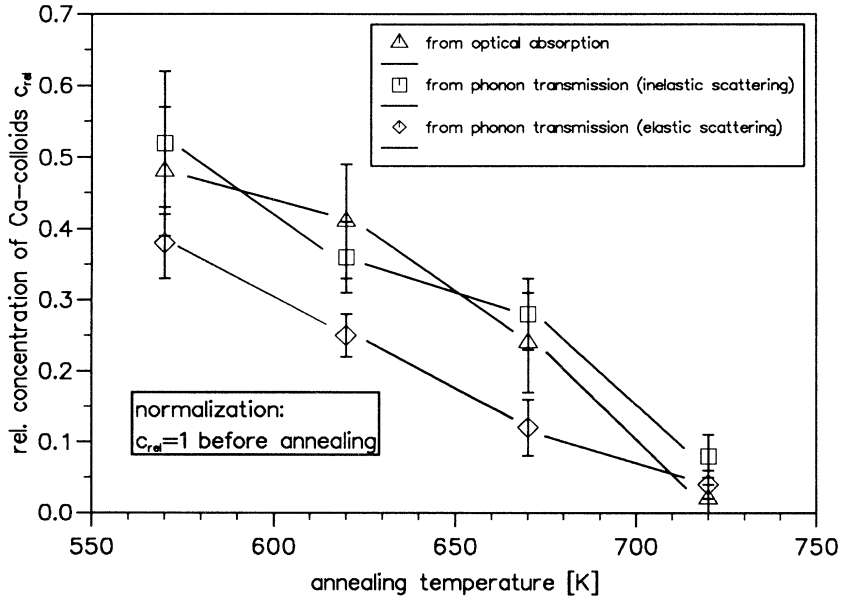

FIG. 3. Relative concentration of Ca clusters after isochronal annealing obtained from optical absorption and phonon transmission spectra. A good correlation is observed assuming inelastic phonon scattering.

tions for the limiting cases of elastic and inelastic scattering to the depth of dip (1) after each annealing step. As pointed out we assume that the average cluster radius and thus the scattering cross section are not changed by annealing. We therefore deduce from these fits the relative change in concentration.

As mentioned above the difference in the functional concentration dependence for both limits allows us to separate elastic from inelastic phonon scattering by comparing the change of the relative concentration of Ca clusters (normalized to the value of the sample before annealing) with the optically obtained values after each annealing step. As shown in Fig. 3 the correlation is better for inelastic than for elastic phonon scattering. This inelasticity could be due to anharmonic processes at the boundary between metallic calcium and the CaF_2 matrix and to dissipation caused by electron-phonon interaction within the metallic Ca cluster.

Since we did not find a FIR absorption at the energy of dip (1) we conclude that there is no electronic transition but an excitation of mechanical modes. To identify the phonon scattering mechanisms associated with the dip at 398 GHz we applied an isotropic continuum model [12, 13] and compared measured and calculated values of resonance frequencies caused by low lying geometric oscillations of the scatterer. We calculated the frequency dependence of the total scattering cross section of an elastic isotropic sphere in an elastic isotropic medium with incident transverse acoustical waves. Since the structure of these clusters is not known the mass density and the elastic constants of bulk Ca were taken [14, 15] for the calculation.

Figure 4 shows the frequency dependence of the normalized scattering cross section $\sigma/\pi a^2$ of the continuum model (A) with the optically obtained average cluster radius $a = 6$ nm and a modified frequency dependence (B) allowing a size distribution of about 25% according to [6]. Additionally we have taken into account the above mentioned losses assuming a Q factor as low as 5. The position as well as the line shape of dip (1) can be thus fitted by reasonable assumptions for the system of Ca clusters.

According to Chassagne *et al.* [16] Ca clusters are preferentially trapped at dislocation loops. In fact, TEM micrographs of an electron-irradiated sample show a high concentration of dislocation loops [17]. We therefore assume that the first step in annealing is a decomposition of dislocation loops into H centers (<111>-oriented F^{2-} molecules). Then if a trapping loop vanishes the free Ca cluster becomes thermodynamically unstable and dissolves rapidly into color centers [18]. H centers and color centers may combine to form relatively stable complexes similar to localized excitons. We tentatively ascribe line (2) at 628 GHz to these complexes. Unfortunately stress experiments were not possible with our thin samples (500 μm) to determine the symmetry of the center.

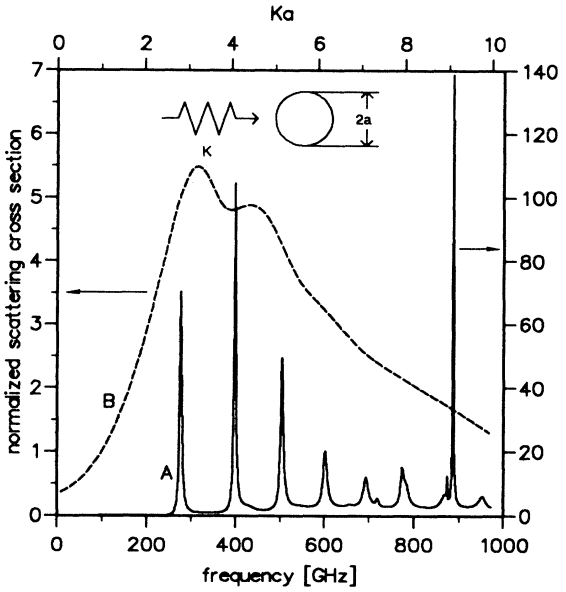

FIG. 4. Calculated frequency dependence of the normalized acoustic scattering cross section of Ca spheres with radius $a = 6$ nm in CaF_2 assuming incident transverse acoustic waves. The upper abscissa gives the dependence in terms of Ka, where K is the TA phonon wave vector. (A): Solution of the continuum model. (B): Additionally including size distribution and damping.

After annealing to 670 K the concentration of color centers starts to decline (see line F at 385 nm [19] in Fig. 2) because their thermal recombination is no more compensated by the increase of concentration in consequence of the decomposition of Ca clusters. The vanishing of free color centers and Ca clusters after annealing at 720 K is accompanied by the dissolution of the localized excitons indicated by the disappearance of dip (2) at 628 GHz (Fig. 1) and by the increase of the absorption line at 308 nm (Fig. 2) associated with free H centers in CaF_2.

Thus by combination of phonon and optical spectroscopy it is shown that electron-irradiation-induced Ca clusters in CaF_2 have a narrow distribution of sizes around 6 nm trapped by dislocation loops also produced by irradiation. This trapping leads to a peculiar annealing behavior in that the radius remains unchanged during the whole process of Ca cluster decomposition due to a stabilization of these clusters by dislocation loops.

We found that Ca clusters scatter phonons resonantly by excitation of mechanical resonances. The resonant phonon scattering at these clusters is strongly damped. As intermediate defects in the annealing process we also found localized excitons in the form of F-H pairs.

We thank M. Forster and H.-E. Schaefer (University of Stuttgart, Institut für Theoretische und Angewandte Physik) for their support during our electron-irradiation

experiments at the Dynamitron accelerator of the Institut für Strahlenphysik, University of Stuttgart. We are grateful to F. Dworschak and his team (Forschungszentrum Jülich, Institut für Festkörperforschung) for performing the low temperature irradiations at the van-de-Graaf accelerator in Jülich. We thank U. Frimmel (University of Stuttgart, 2. Physikalisches Institut) for the optical absorption measurements. We are obliged to U. Buchenau (Forschungszentrum Jülich, Institut für Festkörperforschung) for the reference of the values of the elastic constants of calcium. This work was supported by the Deutsche Forschungsgemeinschaft (DFG).

[1] H. Überall and H. Huang, *Physical Acoustics* (Academic, New York, 1976), Vol. 12, p. 217.
[2] J.M. Worlock, Phys. Rev. **147**, 636 (1966).
[3] K. Guckelsberger and K. Neumaier, J. Phys. Chem. Solids **36**, 1353 (1975).
[4] W. Eisenmenger, *Physical Acoustics* (Ref. [1]), p. 79.
[5] E. Dittrich, W. Scheitler, and W. Eisenmenger, Jpn. J. Appl. Phys. **26**, 873 (1987), Suppl. 26-3.
[6] V.M. Orera and E. Alcalá, Phys. Status Solidi (a) **38**, 621 (1976).
[7] E. Duval, G. Mariotto, M. Montagna, O. Pilla, G. Viliani, and M. Barland, Europhys. Lett. **3**, 333 (1987).
[8] E. Johnson and L.T. Chadderton, Radiat. Eff. **79**, 183 (1983).
[9] C. Wurster, K. Lassmann, and W. Eisenmenger, in Proceedings of the Seventh International Conference on Phonon Scattering in Condensed Matter (Springer-Verlag, Berlin, to be published).
[10] D.V. Kazakovtsev and Y.B. Levinson, Phys. Status Solidi (b) **96**, 117 (1979).
[11] W. Scheitler, thesis, University of Stuttgart, 1989.
[12] N.G. Einspruch, E.J. Witterholt, and R. Truell, J. Appl. Phys. **31**, 806 (1960).
[13] R.J. Mc Bride and D.W. Kraft, J. Appl. Phys. **43**, 4 (1972); **43**, 853 (1972).
[14] M. Heiroth, U. Buchenau, H.R. Schober, and J. Evers, Phys. Rev. B **34**, 6681 (1986).
[15] M. Taut and H. Eschrig, Phys. Status Solidi (b) **73**, 151 (1976).
[16] C. Chassagne, D. Durand, J. Serughetti, and L.W. Hobbs, Phys. Status Solidi (a) **41**, 183 (1977).
[17] C. Wurster, thesis, University of Stuttgart, 1992.
[18] F. Seitz, Rev. Mod. Phys. **26**, 7 (1954).
[19] B.C. Cavenett, W. Hayes, I.C. Hunter, and A. M. Stoneham, Proc. Roy. Soc. London A **309**, 53 (1969).